International Journal of
INTELLIGENT SYSTEMS AND APPLICATIONS IN ENGINEERING
ISSN:2147-6799 www.ijisae.org Original Research Paper

Brain Tumour Segmentation Using Adaptive Deep Convolutional Neural Network System

S. Nandhini Devi[1*], Dr. E. Gnanamanoharan[2], Dr. M. Chinnadurai[3]

Submitted: 22/08/2023 **Revised**: 07/10/2023 **Accepted**: 21/10/2023

Abstract: Major studies in the current area of academic localization are brain tumor segmentation. The focus of the emotional system is diverted to an important organ called the brain. Therefore, deficiency in synchrony causes real and disconnected clinical complications, in which case early diagnosis is seen as an important part. The differentiating evidence of the organization of growth and the area affected by growth is seen as the underlying movement in disease characterization. The need for a mechanized office to study the life structures and defects of the vital element has a definite influence on the different application of solution films. Adaptive Deep Convolutional Neural Network (ADCNN) is a technique developed in this research for brain tumour segmentation. The ADCNN combines Deep Convolutional Neural Network (DCNN) and Remora Optimization Algorithm (ROA). In the DCNN, the optimal learning rate is computed with the help of ROA algorithm. The DCNN method is utilized to the extraction of portions from MRI images. After that, the ROA algorithm is used to select the DCNN's learning rate. The performance of the suggested method is evaluated after its implementation in MATLAB. Performance metrics such as Jaccard Similarity Index (JSI), Dice Similarity Coefficient (DSC), specificity, sensitivity, and accuracy, justify the suggested technique. The proposed method is compared to traditional clustering techniques such as Fuzzy C Means Clustering (FCM), K-Means Clustering, and Convolutional Neural Network (CNN),.

Keywords: *semantic segmentation, brain tumor, convolutional neural network, remora optimization algorithm and MRI images*

1. Introduction

Brain tumours can develop from aberrant cell proliferation inside of the brain or even from cells that have spread to the brain from another malignant growth. There are numerous types of classifications of cerebral cancers that are grouped by their starting cells and depending on their danger and developmental traits, might be categorised as low or high. The best therapy starts with identifying the extent and kind of the cancer. Methods of clinical imaging are used to detect and assess growth. Magnetic resonance imaging (MRI), one of these clinical imaging techniques, is often utilised for clinical decision-making, treatment selection, prognostication, and clinical and radiation plans. There are picture kinds and modifications that improve the radiation rating of the growth type [1] because of the multimodal idea of MRI. Computer support systems have been invented to help with traditional neurological diagnosis and treatment layouts. Image manipulation and machine learning calculations with design approval are commonly used as a handbook for interpreting medical pictures. Segmentation strategies have been recommended for very long-term applications. For cerebral development, the imaging section can help to determine the amount of cancer rapidly and impartially, and to focus on patient obvious features and to organize decision and treatm ent [2,3]. Due to the development of the brain, the precise marking of cancerous tissue and normal mental areas is an essential division task. In general, the location of the growth is not clear on the outside, although it is difficult to pinpoint the exact and reproducible segment and the working disorder in different types of cancer and in different MR scanner types [4]. In fact, even within a neurotic class of cancer, there is an enormous assortment and complexity of developmental imaging characteristics such as image surface and its size, shape, gesture power, and other common cerebral structures [5]. Some cancers of high quality are very diverse and have a necrotic center surrounded by practical development that invades regular mental tissues. Continuous underdeveloped areas may also appear abnormal as areas of edema develop due to a provocative reaction. Therefore, developing an all-encompassing strategy to accurately dissect cancers is a complex task. Clinical requirements for the oncology unit include the area prepared for radiotherapy, evaluating changes in the extent of growth, checking for low- to high-grade changes in the cleft palate, and observing treatment reactions [6].

Manually segmentation cancers on MRI images is difficult and concise because it relies on the expertise and experience of the executives, and then the regeneration between executives is minimal [7,8]. Programmed computer

[1*]*Research Scholar,Department of Electronics and Communication Engineering, Annamalai University, Chidambaram,*
Email id: sjnandhinidevi@gmail.com
[2]*Assistant Professor,Department of Electronics and Communication Engineering,*
Email id: gnanamanohar@gmail.com
[3]*Professor and Head, Department of Computer science and Engineering, E.G.S Pillay Engineering College,*
Email id: mchinnadurai@egspec.org

techniques can give a true segmentation of cancers, and allow large-scale multimodal MRI information to be examined within a prudent handling time. However, manual separation by experts is generally used as the best standard for reviewing programmed or computer-aided section practices and for further framework preparation [9,10].

Main contribution of the research is,

1. ADCNN is developed for brain tumour segmentation. The ADCNN is a combination of DCNN and ROA. In the DCNN, the optimal learning rate is computed with the help of the ROA algorithm.
2. The DCNN method is utilized to the extraction of portions from MRI images. After that, the learning rate of the DCNN is chosen with the assistance of the ROA algorithm. The proposed approach is implemented in MATLAB, and performance is evaluated.
3. Validation of the proposed method by performance metrics such as JSI, DSC, specificity, sensitivity and accuracy.
4. The proposed approach is compared to traditional methods such as CNN, K-Means Clustering and FCM.

The extra portion of the paper is re-arranged as below, and the related work review section is presented in section 2. The projected approach description and steps are given in section 3. The outcome of the results is represented in section 4, and the conclusion of the part is explained in section 5.

2. Related works

Experimental work for the planned brain tumour segmentation has been expanding over the years, which has addressed the interest in this area of research and is currently ongoing. Some techniques have been proposed in writing to identify and segmentation of tumours based on MRI images. A few research methods are examined in the following section.

Mina Ghaffari *et al.* [11] explored an automatic technique for brain tumour segmentation into its subtypes. Fifteen of the patients in the database were treated with postoperative radiation therapy, including manual feedback of their developmental subgroups, including multimodal postutility psychiatric tests (T1 MRI, post-Catolinium T1 MRI and T2-FLAIR images). A 3D dense U-net was developed to separate the brain cancer districts and extensive analyzes were enabled to improve sample accuracy. Abhishta Bhandari *et al.* [12] Introduced Brain Networks for the Mental Cancer Unit. Mental development, especially the glioblastoma multiforme (GBM) is a growing area of interest for examination. The developmental stage is significant in the readiness to go into the analysis of this pathology. The manual division is often contradictory as it varies between eyewitnesses. A mechanized unit was proposed to combat this problem. Strategies, for example, CNNs, machine learning pipelines that display the organic course of neurons (called hubs) and neurotransmitters (associations) are interested in writing. Shanaka Threefold in-depth learning designs have been introduced by Ramesh Gunasekara *et al.* [13]. First, the classifiers are activated with a deep CNN, and second, a region-based CNN (R-CNN) is performed on the images arranged to control the interest development districts. As a third and final step, the concentrated growth threshold for the section cycle is designed using the Chan–Vese segmentation calculation. Dillip Ranjan Nayak *et al.* [14] have introduced an Independent technique for segmenting brain tumours in light of Deep Neural Networks (DNNs). Here, it depicts an exceptional CNN format that differs from what is commonly used in PC viewing. The characteristics of growth cells were an undeniable challenge due to their diversity. From the perspective of visual learning and mental cancer recognition, a CNN is the most widely used AI calculation. Amjad Rehman Khan *et al.* [15] has introduced an in-depth learning approach to dealing with brain tumour, which uses MRI information inquiry to assist specialists. The recommended strategy consists of three main stages: preoperative, psychiatric unit, application of k means clustering, and finally, sorting of MRI information into their individual classifications (harmless / threat) by means of a sophisticated VGG19 (i.e., 19-layer visual geometric panel) model.

3. Proposed System Model

The systematic segmentation of brain tumours is a requirement in the medical field for getting efficient results. In recent years, researchers create several types of approaches to achieve the segmentation of tumors from the input images. Hence, in this study, ADCNN is developed for the segmentation of brain tumours. The ADCNN is a combination of ROA and DCNN. In the DCNN, the optimal learning rate is computed with the help of ROA algorithm. The MRI images are partially extracted using the DCNN algorithm. The ROA algorithm will be employed for selecting the DCNN's learning rate.

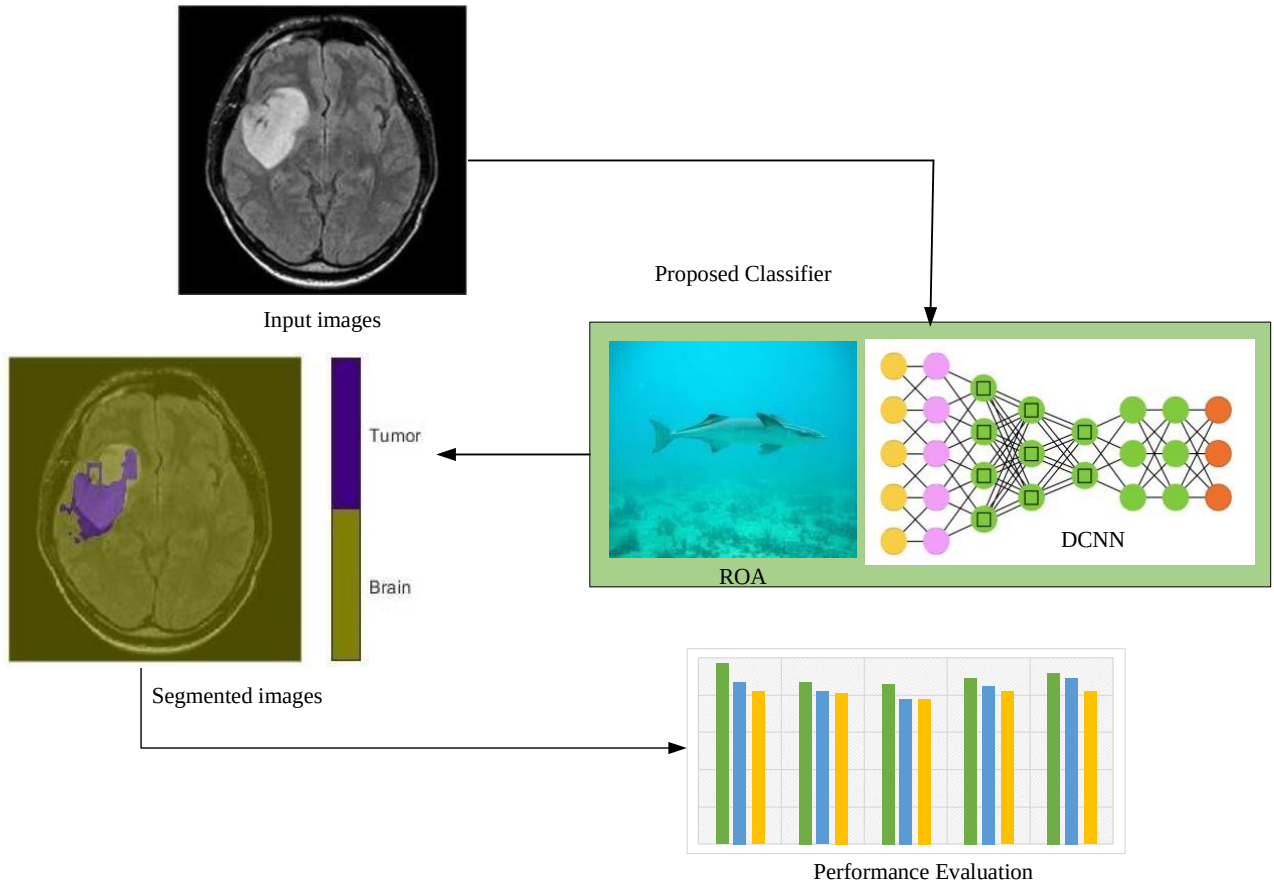

Fig 1: System Architecture.

From the figure 1, initially, the database is gathered from benchmark system. Post that, images are transmitted to the ADCNN classifier in order to segment brain tumors. The detailed explanation of the proposed method is represented in this following section.

3.1. Convolutional Neural Network (CNN)

CNN is the most effectively developed and implemented type of artificial neural network. A multilayer perceptron (MLP) is also a component of a CNN. The activation functions of each individual neuron in the MLP are designed to connect to weighted inputs and the output itself. The deep MLP is used in the design of the MLP, and the network structure is related to the single hidden layer. The CNN can also be an MLP with a unique appearance. Because of the model architecture, the particular design makes it possible for rotation and translation to be invariant. The three basic layers that comprise a CNN architecture when a rectified linear activation function is taken into account are the fully connected layer, the pooling layer, and the convolutional layer [16]. The proposed CNN design comprises three fully linked, max polling and convolutional layers. Each convolution layer (layer 1, layer 3, and layer 5) can use the kernel size consideration, which was developed based on the following formulation.

$$X_N = \sum_{k=0}^{n-1} Y_k F_{N-k} \tag{1}$$

Convolutional processing is used. Here, Y as the input image, N can be interpreted as the number of elements, and F as the filter. The pooling process is then considered for each convolution layer to produce the feature maps. The feature map's size can be decreased to meet the maximum pooling requirement. The ROA technique is used to obtain the kernel size with the parameter, while the convolution stride and max pooling operation are fixed at 1 and 2, respectively. In layers 1, 3, 5, 7 and 8, the activation function in CNN is assumed to be a leaky rectifier linear unit. Hence 5, 20, and 30 output neurons are present in the fully linked layer, which has the designated output layer. The segmented images can be divided into two groups, such as the remaining and segmented portion, using the Softmax max function. Table 1 displays CNN's design specifications.

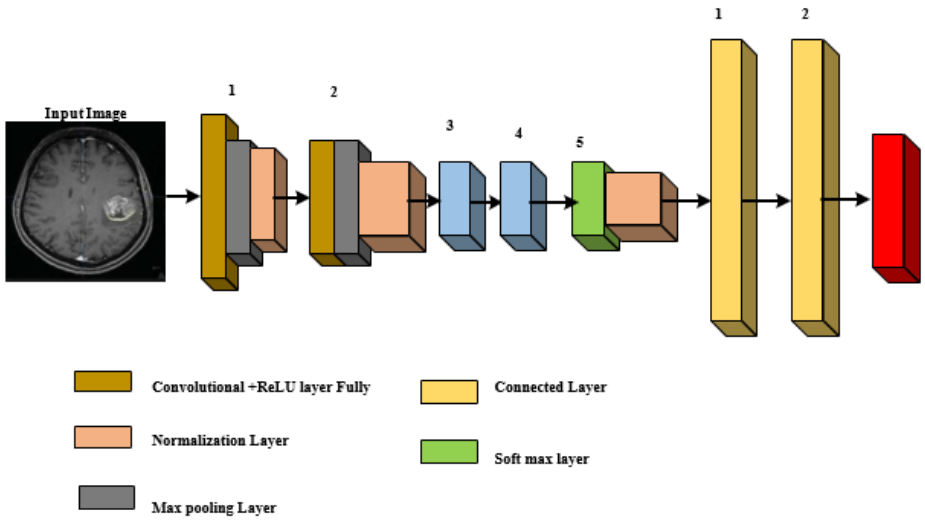

Fig 2: Structure of Convolutional Neural Network

Table 1: CNN parameters

S. No	Layers	Type	Kernel size	Stride	Number of neurons
1	0-1	Convolution	3	1	258*5
2	1-2	Max-Pooling	2	2	129*5
3	2-3	Convolution	4	1	126*10
4	3-4	Max-Pooling	2	2	63*10
5	4-5	Convolution	4	1	60*20
6	5-6	Max-Pooling	2	2	30*20
7	6-7	Fully connected	-	-	30
8	7-8	Fully connected	-	-	20
9	8-9	Fully connected	-	-	5

With the help of the backpropagation method and a sample size of

10, the intended CNN is trained. The CNN's hyper parameters, momentum, learning rate, and regularization, were also regularized with the support of ROA. This parameter controls the speed of the training process, data overfitting and data convergence. To achieve effective results, the settings are modified in accordance with the ROA approach. Additionally, based on the formulation below [17], the weights and biases have been modified.

$$\Delta W_T(T+1) = -\frac{X_\lambda}{R} WL - \frac{X}{N}\frac{\partial c}{\partial WL} + M\Delta WL(T) \quad (2)$$

$$\Delta W_T(T+1) = -\frac{X}{N}\frac{\partial c}{\partial bL} + M\Delta bL(T) \quad (3)$$

Here, W can be defined as weight, T can be defined as updating step, c can be defined as cost function, M can be defined momentum, λ can be defined as regularization parameter, X can be defined as learning rate, b can be defined as bias, L can be defined as layer number and N can be defined as the total number of training set. The CNN is trained and tested over the course of 20 epochs. In the process of training and testing, 80% of the images are used to train the network and the remaining 20% are used to test the network.

3.2. Remora Optimization Algorithm

The ROA is used to select optimal CNN parameters for optimal image segmentation process. Remora can be specific animal which have the ability to swim with different sea creatures, oceangoing hulls in addition whales. This pursuit saves jobs and frees you from enemy attack. It is usually transported in tropical waters, although it follows the host growth of viral water. Remora from invertebrate or fish species. When it comes to the ocean rich in gravity, it relieves from the host, eats the food, and then engrosses it with the new host in addition move on to another ocean. However, sometimes, like a cleaner, it is more conceivable to ectoparasites or eat food that destroy the outside of the transporter. As initialization takes place, the CNN hyperparameters are selected optimally.

3.2.1. Initialization:

The remora optimization algorithm works by assuming that the candidate is a remora. Furthermore, the search location includes position R as a parameter, where the remora is located. The remora swims in dimensional spaces (one-dimensional, two-dimensional, three-dimensional, and super-dimensional), and their position vector changes accordingly. The current position of the remora can be expressed in the following manner.

$$rI = \left(rI_1, rI_2, ..., rI_D\right) \tag{4}$$

The dimension in the search space of remora is denoted as *D*, while *I* be represented as the number of remoras. In the process of searching through the remora search space, the most optimal solution for the optimization algorithm is referred to as the remora's meal. [18].

$$r_{best} = \left(r_1^*, r_2^*, ..., r_D^*\right) \tag{5}$$

In this approach, every potential solution is associated with a fitness function that is specifically described in this case,

$$F\left(rI\right) = F\left(rI_1, rI_2, ..., rI_D\right) \tag{6}$$

$$F\left(r_{best}\right) = F\left(r_1^*, r_2^*, ..., r_D^*\right) \tag{7}$$

In this case, F can be interpreted as the problem's fitness function.

The most optimal position for remora is determined using equation (4) and is used as the storage for the best solutions. Remora is considered to be the most important parameter in computing the answer and can be found scattered throughout the search area. Other marine creatures have their own specific ways of updating location and can be utilized as a means of managing the remora during location updates. Remora has the ability to calculate the best position by considering the search space, and it can operate in either exploration or exploitation mode.

3.2.2. . Fitness Evaluation

Following is a mathematical representation of the fitness function:

$$MSE = \frac{1}{N * M}\sum_{X=1}^{N}\sum_{Y=1}^{M} MSE\left[I_{image}\left(A,B\right) - I_{d-image}\left(A,B\right)\right] \tag{8}$$

$$FF = MAX\left\{PSNR\right\} \tag{9}$$

$$PSNR = 10\log_{10}\left(\frac{MAX^{P}}{MSE}\right) \tag{10}$$

Where $I_{image}\left(A,B\right)$ is referred as an input image and $I_{d-image}\left(A,B\right)$ is defined as segmented images. The DCNN images that are used to improve the best semantic segmentation procedure are chosen based on the fitness function.

3.2.3. Exploration stage

The location of the remora is updated when it is connected to the swordfish. In relation to the sophisticated data of this method, the equation for location updates is improved and is written as follows:

$$r_{IT+1} = r_{bestT} - \left(rand(0,1) * \left(\frac{r_{Tbest}}{2} + r_{R\ and\ T}\right) - r_{R\ and\ T}\right) \tag{11}$$

The definition of $rRand$ is a randomly chosen location, while the maximum number of iterations are denoted by T . The optimal solution is determined by the most suitable location for the remora update. In addition, combining the random selection of remora can enhance the exploration search space. The remora has the ability to choose whether or not to attack certain hosts associated with its prey. The fitness function parameters of the present generation are more efficient than those of earlier generations. The current fitness parameter is calculated based on past attack experiences [19].

3.2.4. Experience Attack

The equation provided calculates the experience attack by using a small step that is associated with the host and is equivalent to the required variation of the host.,

$$r_{attend} = r_I^T + \left(r_I^T - r_{pres}\right) * randn \tag{12}$$

The term " r_{attend} " refers to a preliminary measure, while " r_{pres} " refers to a perspective taken before something is created, which is considered practical. The proposed

solution and the attempted solution's fitness function parameters are compared and evaluated, and the most optimal solution is chosen using the following expression.

$$f\left(r_i^T\right) > f\left(r_{attend}\right) \tag{13}$$

Remora has a range of feeding methods to choose from when it comes to local optimization, and these methods will be further explained in the following section. The proposed solution's fitness function parameter can exceed that of the current solution selected by the host.

$$f\left(r_i^T\right) < f\left(r_{attend}\right) \tag{14}$$

3.2.5. Exploitation Stage

The update of the remora location during the exploitation stage is shown in the equations below.

$$r_{I+1} = d * e^{a^*} \cos(2\pi\alpha) + r_i \tag{15}$$

$$\alpha = Rand(0,1) * (A-1) + 1 \tag{16}$$

$$A = -\left(1 + \frac{t}{T}\right) \tag{17}$$

$$d = \left|r_{best} - r_I\right| \tag{18}$$

If we consider a random variable A that falls within the range of [-1, 1], and we decrease it to the range of [-2, -1], and if we define d as the distance between a prey and a hunter, then we can say that A and d are related..

3.2.6. Host feeding behaviour

Host feeding refers to the act of separating the process of exploitation into distinct sections. During this step, the solution space is narrowed down to the host's location space. Any constraints that arise from moving around or being present within the host's environment may be considered minor issues that are reduced in importance.,

$$r_i^T = r_i^T + A \tag{19}$$

$$A = b * \left(r_i^T - c * r_{best}\right) - V \tag{20}$$

$$V = 2 * \left(1 - \frac{t}{Maximum\ iteration}\right) \tag{21}$$

A can be referred as a minor variation that is linked to the volumes of both the host and the remora. The factor c of the remora was utilized to restrict the position of the remora in order to determine the location of both the host and the remora within the search space.

3.2.7. Computational Complexity

The level of challenge involved in the method can be illustrated by considering factors such as the highest number of iterations, dimensions, and remoras needed to confirm the ROA. The absence of a sorting mechanism may not have a significant impact.

The notation "o(n)" is used to represent the complexity of the technique. The complete expression for the complexity is given below,

$$o(roa) = o(fitness\ function) * \left(o(initialization) + o(\exp loration) + o(\exp loitation)\right) \tag{22}$$

$$= o\left(f(r) * o\left(t * \left(o(n)\right) + o(n*t*d) + o\left(o(n*t*d)\right)\right)\right) \tag{23}$$

$$= o\left(f(r)\right) * o\left(n * (td+1)\right) \tag{24}$$

The complexity is represented as $o\left(f(r)\right)$, which is related to the fitness function. For the exploration stage, computational complexity is indicated as $o(n,t,d)$, while for the exploitation stage, it is written as $o(n*t*d)$.

4. Results and discussion

This section presents the justification and validation of the projected approach. The projected approach is validated with the consideration of performance measure. To justify the proposed method, it is implemented in MATLAB software R2016b. It has 6GB RAM and a laptop with an Intel Core i5-2450M 2.50GHz processor. The proposed approach is executed considering standard benchmark dataset [20]. This collected database consists of 253 images. The implemented approach is analyzed with the accuracy, DSC, JSC, sensitivity and specificity in the segmentation of brain tumours. The projected approach is developed to isolate the tumour from MRI pictures. The simulation parameters of the projected approach are depicted in table 2.

Table 2: Simulation Variables

S. No	Approach	Parameters	Value
1	Proposed approach	Lower bound	-10
2		Upper bound	10
3		Number of populations	100
4		Maximum number of iterations	100
5		Number of Decision Variables	5

The performance metrics are computed based on the definition below to justify the projected approach.

- A brain tumor is efficiently segmented from the MRI image is defined as True Positive (TP)
- A brain tumor is not effectively segmented and not corrected; it is defined as True Negative (TN)
- A brain tumor is not segmented, which defined as False Positive (FP)
- A brain tumor is segmented but not corrected, defined as False Negative (FN).

Based on the above formulation, the projected approach is calculated using the equations below.

Accuracy:

$$Accuracy = \frac{TN + TP}{TN + FP + TP + FN} \tag{25}$$

Sensitivity:

$$\text{Re}\,call = \frac{TP}{(TP + FN)} \tag{26}$$

Specificity:

$$Specificity = \frac{TN}{(TP + FP)} \tag{27}$$

DSC and JSI: It is a similarity index variable formulated as follows,

$$DSC = 2\frac{|S \cap G|}{|S + G|} \tag{28}$$

$$JSI = 2\frac{|S \cap G|}{|S \cup G|} \tag{29}$$

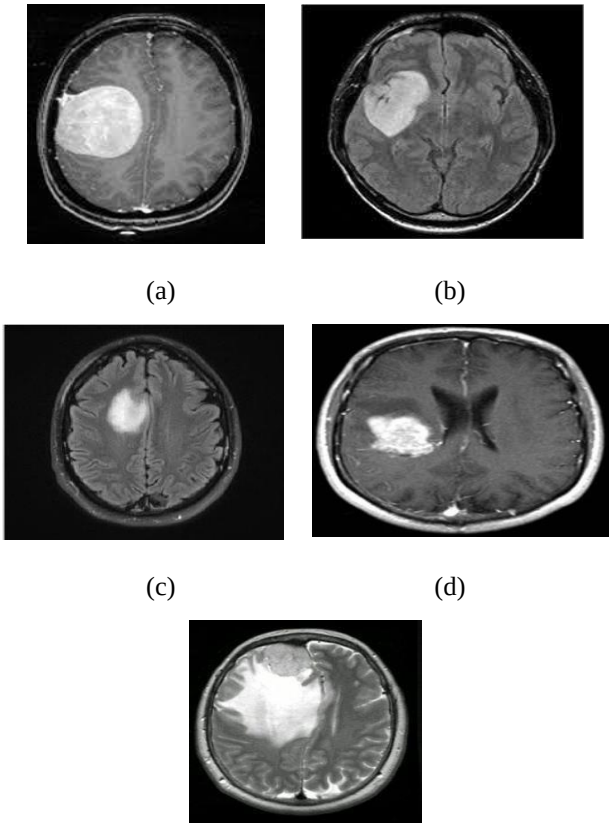

(a) (b) (c) (d) (e)

Fig 3: MRI input images

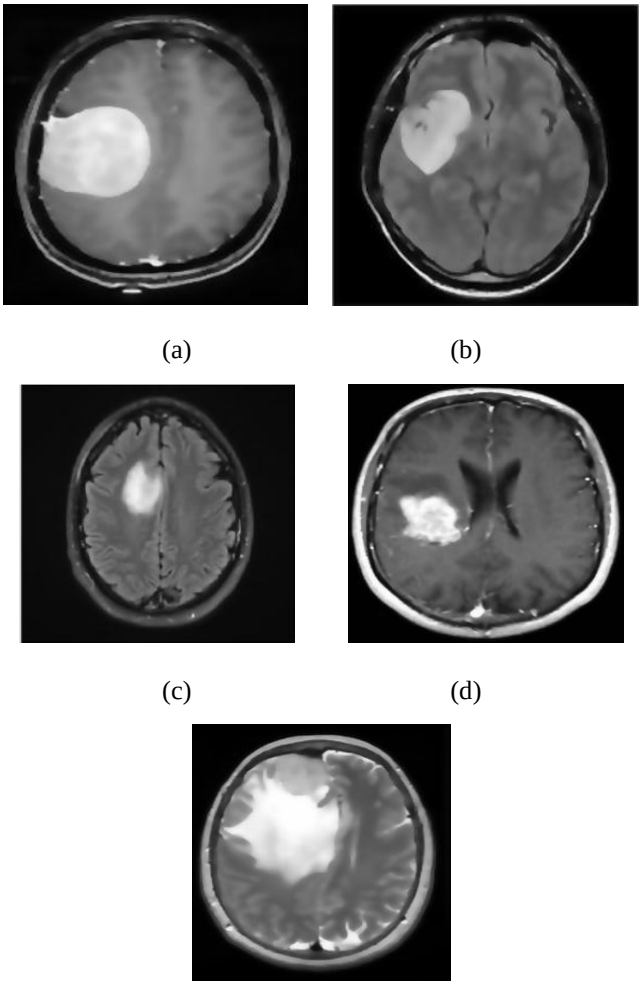

(a) (b)

(c) (d)

(e)

Fig 4: Pre-processing images

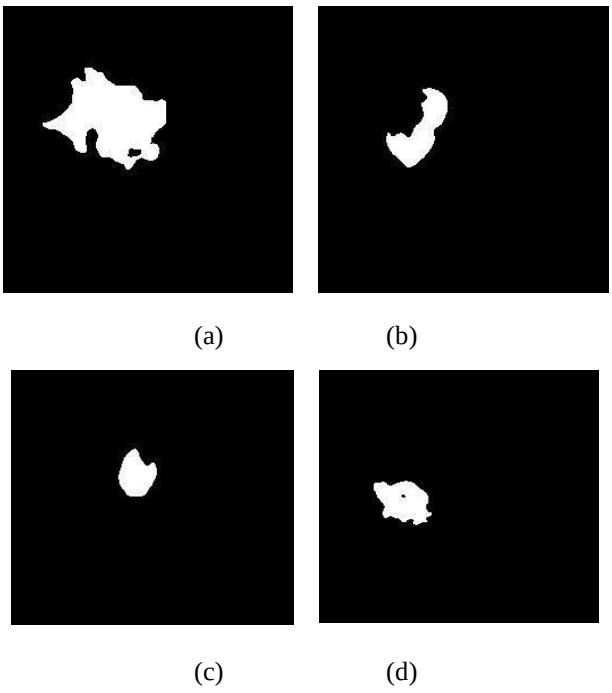

(a) (b)

(c) (d)

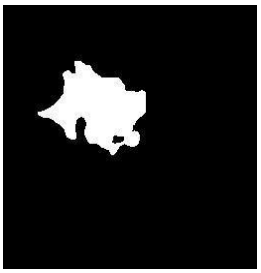

(e)

Fig 5: Segmented images

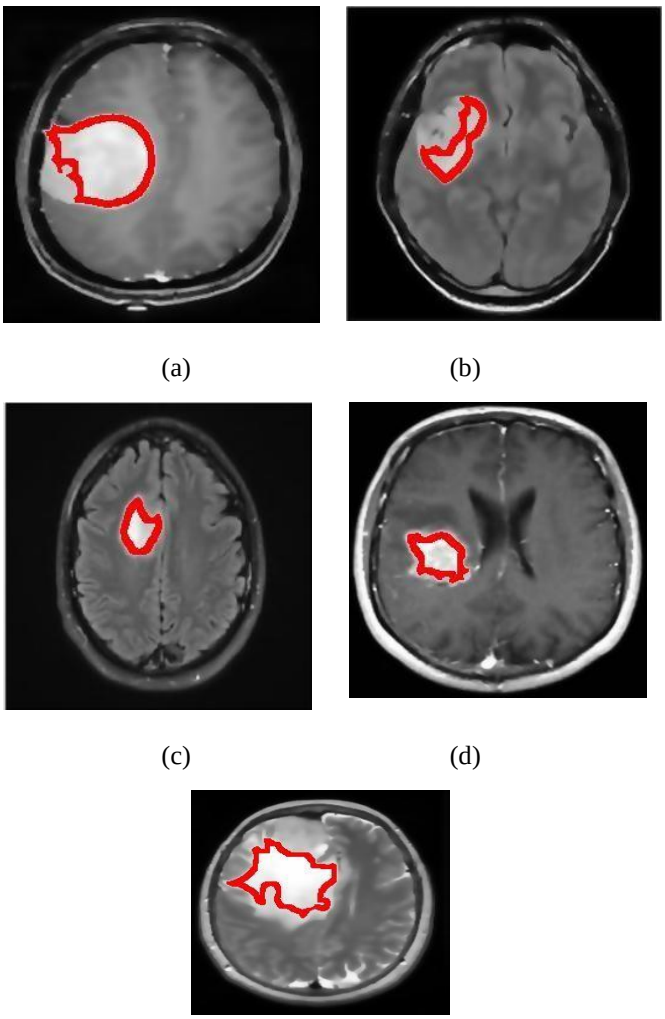

(a) (b)

(c) (d)

(e)

Fig 6: Tumor outlined images

The sample input database images are presented in figure 3. After that, the pre-processing images are shown in figure 4. Figures 5 and 6 exhibit tumour outlined and segmented images, respectively. The DSC measure is a similarity measure parameter that is utilized to validate the projected approach. The DSC measure of the implemented approach is evaluated and illustrated in figure 7(a). The suggested approach is contrasted with the conventional approaches such as CNN, FCM, K-Means clustering. The projected approach can be attained the 0.98 DSC measure for the first image.

Similarly, the CNN approach can be attained the 0.94 DSC measure for the first image. The FCM approach can be attained the 0.91 DSC measure for the first image. the K-means clustering approach can be attained the 0.87 DSC measure for the first image. The JSI measure of the intended approach is evaluated and depicted in figure 7(b). The proposed approach contrasts conventional techniques such as CNN, FCM, K-Means clustering.

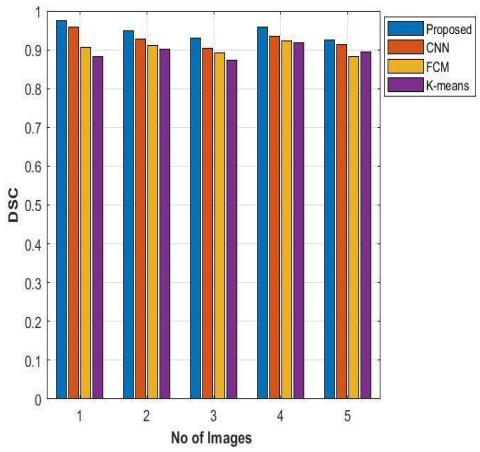

(a)

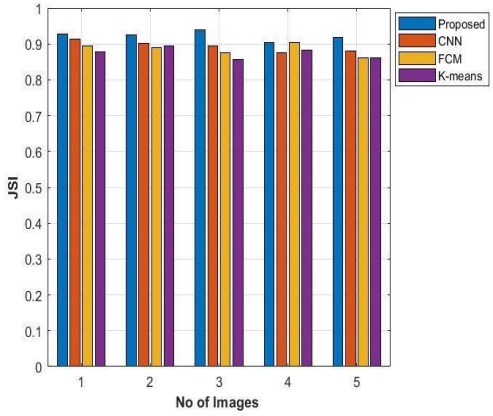

(b)

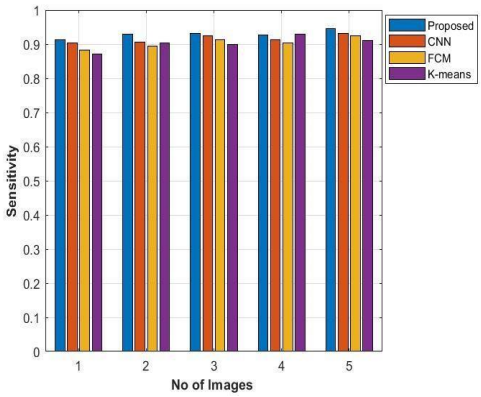

(c)

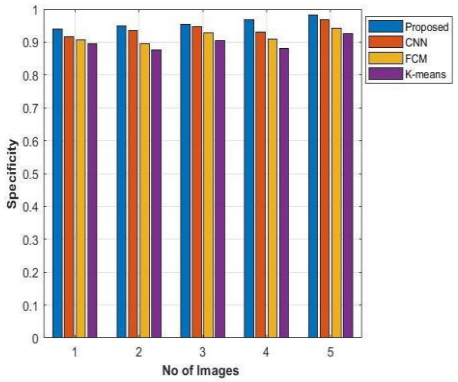

(d)

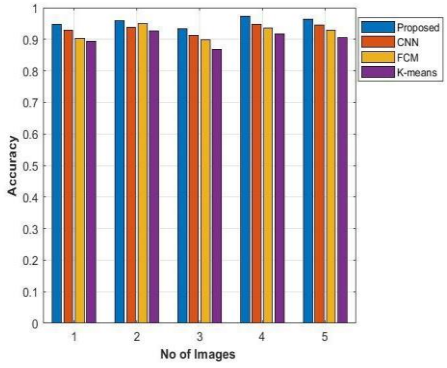

(e)

Fig.7: Output of (a)DSC, (b) JSI, (c) Sensitivity, (d) Specificity, and (e) Accuracy

The sensitivity and specificity measure are a performance measure parameter which is utilized to validate the projected approach. The sensitivity measure of the intended approach is evaluated and exhibited in figure 7(c and d). The proposed method is contrasted with the conventional approaches such as CNN, FCM, K-Means clustering. The projected approach can be attained the 0.92 specificity measure for the first image. Similarly, the CNN approach can be attained the 0.90 specificity measure for the first image. The accuracy measure is a performance measure

parameter which is utilized to validate the projected approach. The accuracy measure of the proposed approach is evaluated and displayed in figure 7(e). The implemented approach is contrasted with the conventional approaches such as CNN, FCM, K-Means clustering. The projected approach can be attained the 0.95 accuracy measure for the first image. Related on the analysis, the suggested technique can be attained optimal solutions in brain tumour segmentation process.

5. Conclusion

In this paper, ADCNN has been generated for brain tumour segmentation. The ADCNN is a combination of ROA and DCNN. In the DCNN, the optimal learning rate is computed with the help of ROA algorithm. To extract portions of the MRI images, the DCNN approach is used. Following that, the ROA algorithm is used to select the DCNN's learning rate. The proposed method is implemented in MATLAB and performance is evaluated. Performance metrics including JSI, DSC, specificity, sensitivity, and accuracy are used to validate the suggested approach. The proposed approach is compared with conventional techniques like CNN, FCM, and K-Means Clustering. According to the analysis, the proposed approach has been achieved efficient results in terms of JSI, DSC, specificity, sensitivity, and accuracy. In future, real time data will be analyzed with the brain tumor segmentation with the consideration of efficient results.

References

[1] Mohammadreza Soltaninejad, Guang Yang, Tryphon Lambrou, Nigel Allinson, Timothy L. Jones, Thomas R. Barrick, Franklyn A. Howe, and Xujiong Ye. "Supervised learning based multimodal MRI brain tumour segmentation using texture features from supervoxels." Computer methods and programs in biomedicine 157 (2018): 69-84.

[2] Zaka Ur Rehman, Syed S. Naqvi, Tariq M. Khan, Muhammad A. Khan, and Tariq Bashir. "Fully automated multi-parametric brain tumour segmentation using superpixel based classification." Expert systems with applications 118 (2019): 598-613.

[3] Sunil Maharjan, Abeer Alsadoon, P. W. C. Prasad, Thair Al-Dalain, and Omar Hisham Alsadoon. "A novel enhanced softmax loss function for brain tumour detection using deep learning." Journal of neuroscience methods 330 (2020): 108520.

[4] Konstantinos Kamnitsas, Christian Ledig, Virginia FJ Newcombe, Joanna P. Simpson, Andrew D. Kane, David K. Menon, Daniel Rueckert, and Ben Glocker. "Efficient multiscale 3D CNN with fully connected CRF for accurate brain lesion segmentation." Medical image analysis 36 (2017): 61-78.

[5] Pawel Szwarc, Jacek Kawa, Marcin Rudzki, and Ewa Pietka. "Automatic brain tumour detection and neovasculature assessment with multiseries MRI analysis." Computerized Medical Imaging and Graphics 46 (2015): 178-190.

[6] Mohammad Havaei, Axel Davy, David Warde-Farley, Antoine Biard, Aaron Courville, Yoshua Bengio, Chris Pal, Pierre-Marc Jodoin, and Hugo Larochelle. "Brain tumor segmentation with deep neural networks." Medical image analysis 35 (2017): 18-31.

[7] A. Selvapandian, and K. Manivannan. "Fusion based glioma brain tumor detection and segmentation using ANFIS classification." Computer methods and programs in biomedicine 166 (2018): 33-38.

[8] Pim Moeskops, Jeroen de Bresser, Hugo J. Kuijf, Adriënne M. Mendrik, Geert Jan Biessels, Josien PW Pluim, and Ivana Išgum. "Evaluation of a deep learning approach for the segmentation of brain tissues and white matter hyperintensities of presumed vascular origin in MRI." NeuroImage: Clinical 17 (2018): 251-262.

[9] Vasupradha Vijay, A. R. Kavitha, and S. Roselene Rebecca. "Automated brain tumor segmentation and detection in MRI using enhanced Darwinian particle swarm optimization (EDPSO)." Procedia Computer Science 92 (2016): 475-480.

[10] Eser Sert, Fatih Özyurt, and Akif Doğantekin. "A new approach for brain tumor diagnosis system: Single image super resolution based maximum fuzzy entropy segmentation and convolutional neural network." Medical hypotheses 133 (2019): 109413.

[11] Mina Ghaffari, Gihan Samarasinghe, Michael Jameson, Farhannah Aly, Lois Holloway, Phillip Chlap, Eng-Siew Koh, Arcot Sowmya, and Ruth Oliver. "Automated post-operative brain tumour segmentation: A deep learning model based on transfer learning from pre-operative images." Magnetic resonance imaging 86 (2022): 28-36.

[12] Abhishta Bhandari, Jarrad Koppen, and Marc Agzarian. "Convolutional neural networks for brain tumour segmentation." Insights into Imaging 11, no. 1 (2020): 1-9.

[13] Shanaka Ramesh Gunasekara, H. N. T. K. Kaldera, and Maheshi B. Dissanayake. "A systematic approach for MRI brain tumor localization and segmentation using deep learning and active contouring." Journal of Healthcare Engineering 2021 (2021).

[14] Nayak, Dillip Ranjan, Neelamadhab Padhy, Pradeep Kumar Mallick, Dilip Kumar Bagal, and Sachin

Kumar. "Brain Tumour Classification Using Noble Deep Learning Approach with Parametric Optimization through Metaheuristics Approaches." Computers 11, no. 1 (2022): 10.

[15] Khan, Amjad Rehman, Siraj Khan, Majid Harouni, Rashid Abbasi, Sajid Iqbal, and Zahid Mehmood. "Brain tumor segmentation using K-means clustering and deep learning with synthetic data augmentation for classification." Microscopy Research and Technique 84, no. 7 (2021): 1389-1399.

[16] Acharya, U. Rajendra, Shu Lih Oh, Yuki Hagiwara, Jen Hong Tan, Muhammad Adam, Arkadiusz Gertych, and Ru San Tan. "A deep convolutional neural network model to classify heartbeats." Computers in biology and medicine 89 (2017): 389-396.

[17] Jin, Kyong Hwan, Michael T. McCann, Emmanuel Froustey, and Michael Unser. "Deep convolutional neural network for inverse problems in imaging." IEEE Transactions on Image Processing 26, no. 9 (2017): 4509-4522.

[18] Jia, Heming, Xiaoxu Peng, and Chunbo Lang. "Remora optimization algorithm." Expert Systems with Applications 185 (2021): 115665.

[19] Almotairi, Khaled H., and Laith Abualigah. "Hybrid Reptile Search Algorithm and Remora Optimization Algorithm for Optimization Tasks and Data Clustering." Symmetry 14, no. 3 (2022): 458.

[20] https://www.kaggle.com/navoneel/brain-mri-images-for-brain-tumor-detection

[21] Goar, V. ., Yadav, N. S. ., & Yadav, P. S. . (2023). Conversational AI for Natural Language Processing: An Review of ChatGPT. International Journal on Recent and Innovation Trends in Computing and Communication, 11(3s), 109–117. https://doi.org/10.17762/ijritcc.v11i3s.6161

[22] Samad, A. . (2022). Internet of Things Integrated with Blockchain and Artificial Intelligence in Healthcare System. Research Journal of Computer Systems and Engineering, 3(1), 01–06. Retrieved from https://technicaljournals.org/RJCSE/index.php/journal/article/view/34